Report on

Feasibility Study of Crystalline Beam Formation in COSY

I.Meshkov, A.Smirnov, A.Sidorin
JINR, Dubna, Russia

J.Stein, J.Dietrich
FZJ, Juelich, Getmany

Abstract

This report describes the numerical simulation of the crystalline proton beam formation in COSY [1] using BETACOOL code [2] and results of experimental investigations of the cooling process at extremely low proton beam intensity.

The numerical studies include the description of experimental results at NAP-M [3] storage ring where the large reduction of the momentum spread was firstly observed. The present simulation shows that this behavior of proton beam can not be explained as ordering state of protons. The numerical simulation of crystalline proton beams was done for COSY parameters. The number of protons when the ordering state can be observed is limited by value 10^6 particles and momentum spread has to be less then 10^{-6}.

During the experiments performed in August 2005 the methods of the beam parameter measurement at low intensity were developed and tested. The minimum equilibrium momentum spread of 10^{-6} at proton number from 10^4 to 10^5 was achieved, which is closed to transition point to the ordered state. Sudden reduction of the momentum spread was not observed and more probably that the equilibrium is determined by effective electron velocity spread in beam.

Contents

1. Introduction

The idea of utilization of an ion beam crystalline state for nuclear physics experiments has a large interest now. The achievement of very low ion temperature in the beam rest frame gives new possibilities in the accelerator physics. First off all it is related to a precise mass measurements based on very small momentum spread of the beam in the ordered state. Other possible application of the ordered beam has an aim to increase the luminosity in the electron-ion collider using the ion beam at relatively high linear density and very small transverse dimensions.

Main advantage of an use of an ion ordered beam in a collider appears when one deals with a beam of rare and/or short-lived nuclides, polarized beams of a poor intensity either of antiprotons. This advantage is related with reduction of the ion beam transverse dimensions after transition to the ordered state. In the normal (gaseous phase) state of the beam the equilibrium transverse emittance is scaled with the particle number as $\varepsilon_{x,y} \propto N^{0.6}$ and the beam cross-section in the collision point slow depends on the beam intensity. The transition to the ordered state with decrease of the particle number leads to sudden reduction of the beam cross-section by a few orders of magnitude. General physical limitation of the collision luminosity is determined by beam-beam effect and maximum luminosity value is restricted by achievable beam-beam parameter. The hope to increase the beam-beam parameter value relates to the fact, that the ion velocities in the ordered state lie near the maximum of the friction force providing by the electron cooling system. Therefore, the diffusion due to beam-beam instability can be suppressed more efficiently.

In the frames of FAIR project the utilization of ordered ion beams can be discussed for electron-ion collisions at New Experimental Storage Ring and for collisions of polarized antiproton and proton beams in PAX experiment. For example one can estimate the expected luminosity gain in the case of ion-electron collisions.

In the ordered state the ion beam transverse dimensions are sufficiently smaller than the electron beam ones and the luminosity of collisions can be estimated as

$$L = \frac{N_{i,tot} N_e f_{rev}}{4\pi \cdot \sigma_\perp^2} \tag{1.1}$$

where $N_{i,tot}$ the total ion number in the ring, N_e is the electron number in the electron bunch, $\sigma_\perp$ is the electron bunch transverse size. This formula can be rewritten using definition of the beam-beam parameter for the ion beam:

$$\xi_i = \frac{Z}{A} \frac{N_e r_p \beta_i^*}{4\pi \beta_i \gamma_i \sigma_\perp^2} \tag{1.2}$$

as follows

$$L = \frac{A}{Z} \frac{N_{i,tot} f_{rev}}{r_p \beta_i^*} \gamma_i \beta_i \xi_i \,. \tag{1.3}$$

In these formulae it was taken into account that electron velocity is close to the speed of light. β_i and γ_i are the ion relativistic parameters, β_i^* is the beta function of the ion ring in the collision point, r_p – classical proton radius. The ξ_i parameter is a linear part of the ion beam betatron tune shift and this tune shift can be compensated by the ring optics. When the ξ_i parameter exceeds some threshold value the beam-beam instability is excited that leads to diffusional increase of the ion beam emittance. Theory explanation of the beam-beam effect given in [4] relates this diffusion

to a non-linearity of the electron bunch electric field and presence of a noise in the storage ring. The diffusion coefficient D can be expressed from the noise relative amplitude u as follows:

$$D = \pi^2 (\xi_i u)^2 \left(\frac{\sigma_{i\perp}}{2\sigma_{e\perp}} \right)^2 . \tag{1.4}$$

The noise amplitude can be estimated by fitting of experimental results and it lies in the range of 0.05 – 0.5.

In the "gaseous" state of the ion beam the electron and ion beam radii in the collision point has to be approximately equal each other to obtain maximum luminosity value. If the ion beam is in the ordered state its transverse dimensions are sufficiently smaller than the electron beam ones. Due to this fact the diffusion will be sufficiently suppressed and the same diffusion power corresponds to significantly larger value of the beam-beam parameters. Increase of the beam-beam parameter can be provided by increase of the electron bunch intensity or by decrease its transverse dimensions in the collision point. Maximum achieved beam-beam parameter at hadron colliders without cooling application is about $5 \cdot 10^{-3}$. The cooling application for the ion beam in gaseous state permits to hope to increase the beam-beam parameter by one order of magnitude at least. In the ordered state of the ion beam the expected threshold beam-beam parameter value lies between 0.2 and 0.5, that corresponds to luminosity increase by one order of magnitude in comparison with the gaseous state.

Thus the maximum achievable luminosity in electron collisions with ordered ion beam is determined on the one hand by threshold beam-beam parameter value and maximum linear density of the ions in the ordered state from the other hand. Theory limit of the maximum ion linear density is related to transition of the beam to zigzag structure [5] and the maximum attainable number of the ions N_{th} is the following:

$$N_{th} = \left(\frac{16\pi^2 Q \Delta Q C \gamma_i^5 \beta_i^2}{7\zeta(3) r_{ion}} \right)^{1/3} , \tag{1.5}$$

where $\zeta(3) = \sum_{l=1}^{\infty} 1/l^3 = 1.2020569$ i is the Riemann zeta function, ΔQ is the maximum possible tune shift, C is the ion ring circumference.

Required luminosities for different studies at NESR in e-IR collider mode of operation are presented in the Table 1 [6]. The luminosities are indicated assuming 2π acceptance of the spectrometer. Values given in square brackets indicate required luminosities using two conventional spectrometers of MAMI A type. The values given in italics exceed the achievable luminosities at the design NESR parameters.

Expected intensity of the RI beam depends on production rate at the target and ratio between the nuclei life-time and period of the storage process. Typical yield at the production target lies in the range from 10^{-7} – 10^{-5} and at primary uranium beam of 10^{12} ions this corresponds to 10^5 – 10^7 radioactive ions per pulse. The maximum stacking duration is limited by the ion life-time and for long lived isotopes the maximum intensity of the stored beam can reach the level 10^7 - 10^{11}. For exotic nuclei the production rate can be sufficiently less – down to a few thousands per pulse. In this case the expected intensity of the stored beam can be of the order of 10^6 or even less.

Table 1. Required luminosities for different studies at e-RI collider.

Reaction	Deduced quantity	Target nuclei	Luminosity $1/[cm^2 sec]$
Elastic scattering at small q	rms charge radius	Light	10^{26} $[3\times10^{26}]$
First minimum in elastic form-factor	Charge-density distribution with 2 parameters.	Light	10^{28} $[10^{29}]$
		Medium	10^{26} $[7\times10^{26}]$
		Heavy	10^{24} $[5\times10^{24}]$
Second minimum in elastic form-factor	Charge-density distribution with 3 parameters.	Medium	10^{29} $[10^{30}]$
		Heavy	10^{26} $[8\times10^{26}]$
Giant resonance	Strength, position, width, decay channels.	Medium and heavy	10^{28} $[7\times10^{28}]$
Quasi-elastic scattering	Momentum distribution, spectral function.	Light	10^{29} $[2\times10^{30}]$

Expected luminosity of e-RI collider given in [7] is presented in the Fig. 1. The luminosity was calculated for the ions at A/Z = 2.587 , number of bunches in the electron ring is 8, the electron number in the electron bunch is $5 \cdot 10^{10}$ at high ion beam intensity and increases by one order of magnitude al low ion beam intensity, number of the ion bunches in NESR is 40. The red line corresponds to the constant beam-beam parameter ξ_i = 0.045. Three upper horizontal lines correspond to a limitation due to the space charge effect for different ion species, namely for Z=3 (dashed dotted purple), Z=28 (dashed green), Z=92 (dotted blue).

For the ion beam intensities below 10^9 the ion beam cross-section determined by equilibrium between electron cooling and intrabeam scattering begins to be less than the achievable electron beam one. In this situation the beam-beam threshold for the ion beam can be much higher and the electron bunch intensity can be increased in accordance with the decrease of the ion beam emittance. The black dashed line in the Fig. 1 shows this additional luminosity benefit due to higher ξ_i value when the ion beam is in the normal state. In the normal state when the ion number decreases below 10^6 the luminosity decreases below 10^{26} $cm^{-2}s^{-1}$ that is not enough to perform investigation of the charge distribution inside nuclei (Table 1).

The transition of the ion beam into the ordered state can occur at the ion beam intensity between 10^5 and 10^6 ions in the ring (formula 1.5). The transition leads to sudden reduction of the ion beam cross-section and electron bunch intensity can be increase by a few times after it. The luminosity after transition increases in accordance with the reduction of the ion beam emittance. The solid black line in the Fig. 1 shows the luminosity benefit due to transition into the ordered state.

Thus, utilization of the ion beam ordered state in the electron–ion collider permits to keep luminosity at the level required for measurements of charge-density distribution even at the ion beam intensity of about 10^5 particles.

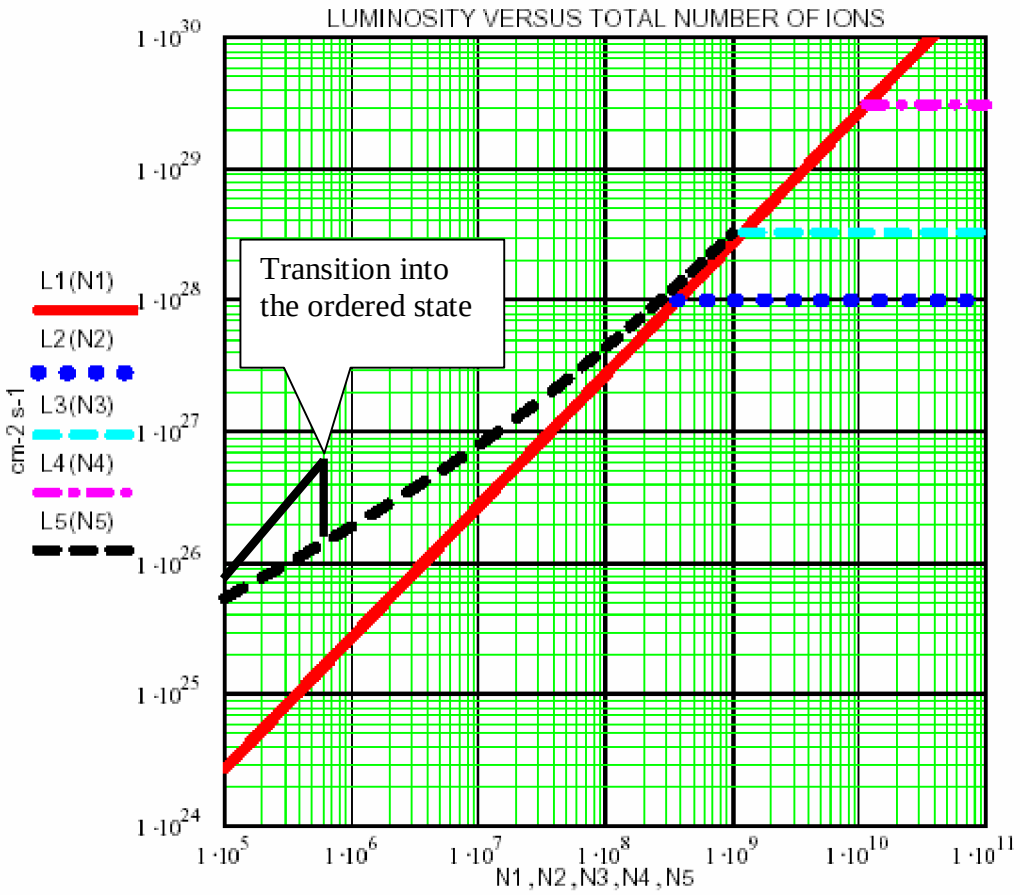

Fig. 1. Luminosity dependence on the ion number. Solid red line corresponds to the constant beam-beam parameter ξ_i = 0.045. Three upper horizontal lines correspond to a limitation due to the space charge effect for different ion species. Black dashed line shows the luminosity benefit due to higher ξ_i at decrease of the ion beam emittance. The solid black line – luminosity after transition into the ordered state.

The effects, which can be interpreted as an ordering of circulating ion beams, were observed at a few storage rings: NAP-M (Budker INP, Novosibirsk), ESR [8] and SIS [9] (GSI, Darmstadt), CRYRING [10] (Stockholm) and PALLAS [11] (München). The particle number in the ordered state observed in experiments is about 3 orders of magnitude less than limiting number (1.5). However, resent experiments with bunched ordered beam performed at ESR and CRYRING shown that the ordered state (after its formation at small ion linear density) keeps the stability after increase the density by the beam bunching.

To explain the discrepancy between theory and experiment the process of the ion beam ordering in ESR storage ring was simulated using BETACOOL program. The simulations showed a good agreement with experimental results and theory of intrabeam scattering in the gaseous state of the ion beam and indicated a few specific peculiarities of intrabeam scattering in transition region between gaseous and ordered states. On the basis of the numerical simulations the new strategy of the cooling process was proposed [12, 13]. The strategy presumes formation of required ratio between transverse and longitudinal beam phase volumes and permits to increase by few times the linear density of the ordered ion beam.

The maximum proton number in the ordered state at COSY estimated in accordance with (1.5) is equal to about 10^6, which permits to test different strategies of the ordered state formation. Experiments at COSY are most important for investigation of possibility to form antiproton ordered beam, because since BINP experiment no attempt to form a proton (antiproton) ordered beam in a cooler storage ring was done.

The goal of experiments described in this report was to develop methods of measurements of a small beam intensity, momentum spread and to test different possibilities of transverse beam heating.

2. Theoretical study of crystalline beam

2.1. Simulation of NAP-M experiments

The dependence of momentum spread of a cooled ion beam has very specific character: at certain conditions the momentum spread drops down to very low value and remains constant with the decrease of the ion beam intensity.

For the first time such a “disappearance” of the beam momentum spread was observed in experiments on NAP-M, where the suppression of the Schottky noise of the cooled proton beam down to very low level was registered (Fig.2.1) [3]. Then the assumption of some orderliness of the cooled beam was declared and soon the idea of the crystalline beam was proposed [14].

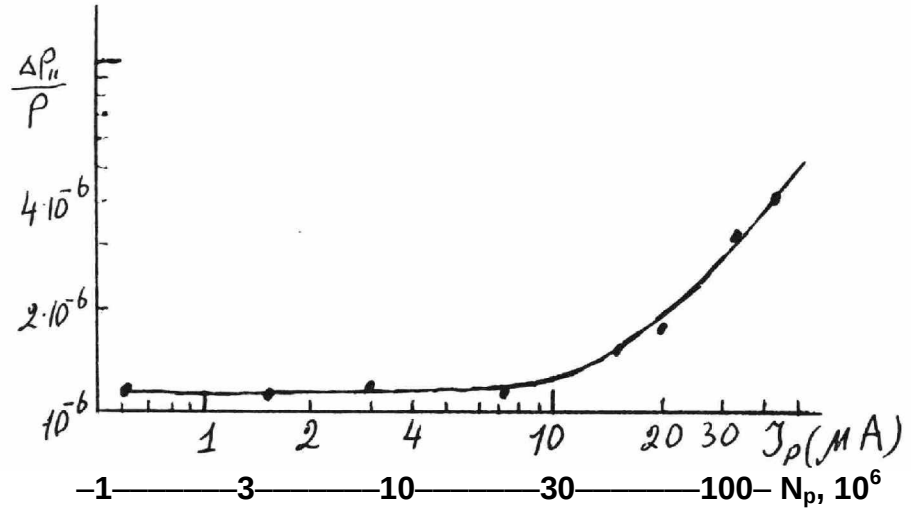

Fig.2.1. NAP-M experiment (1979).
The dependence of momentum spread on proton number (1 μA = $2{,}64 \cdot 10^6$ protons).

To verify the idea of ordering proton beam in NAP-M the numerical simulation of beam dynamics was done for NAP-M lattice structure (Fig.2.2) which was reconstructed from original articles. The main parameters of NAP-M are presented in Table 2.1. The example of input file for MAD program is the following:

```
drift1: drift, l=7.1
sbend1: SBEND, L=4.7124, ANGLE=1.5708, E1=0.415, E2=0.415
NAPM: line=(drift1,sbend1,drift1,sbend1,drift1,sbend1,drift1,sbend1)
```

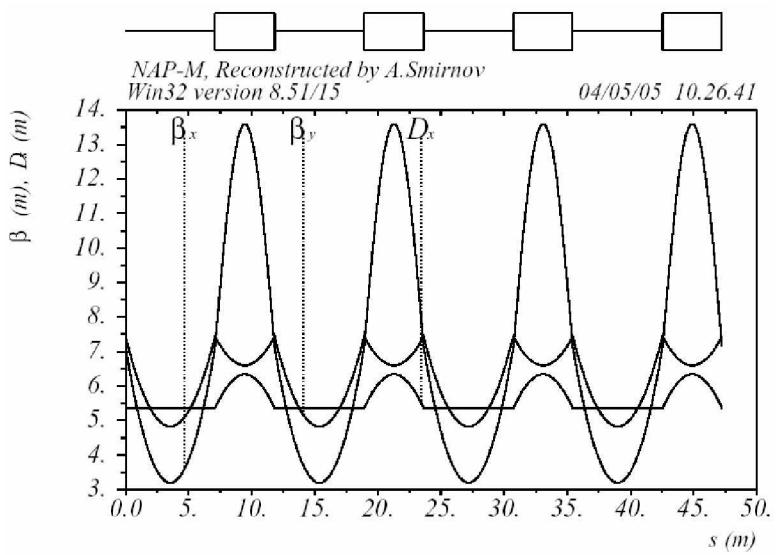

Fig.2.2. Lattice structure of NAP-M.

Table 2.1. Parameters of NAP-M.

Circumference, m	47,25
Proton energy, MeV	65
Transition energy, γ_{tr}	1,069
Betatron tunes, Q_x/Q_y	1,34 / 1,24
Dipole field stability	$\sim 10^{-5}$
Electron cooler	
Cooling section length, m	1,0
Beam current, A	0 ÷ 1,0
Beam radius, cm	0,5
Magnetic field, kG	1,0
Electron energy stability	$\sim 10^{-5}$

Fig.2.3. shows the result of simulation for NAP-M using RMS Dynamics algorithm for proton number 10^6 and electron beam current 1A. IBS heating growth rates are calculated with Martini model.

Fig.2.4 shows the result of simulation for NAP-M using Molecular Dynamics algorithm for proton number 10^6 and 2×10^6 with constant cooling rates of 20 μsec. Ordering state exist for particle number of 10^6 only.

Overlapping transverse and longitudinal components of IBS (Fig.2.4,e,f) one can find the particle number when the ordering state can be reached. In the case of particle number 10^6 the summary pictures (Fig.2.4,e) has the channel between heating growth rates. The simulation results using Molecular Dynamics technique show (Fig.2.4,e) that the proton beam can reach the ordered state.

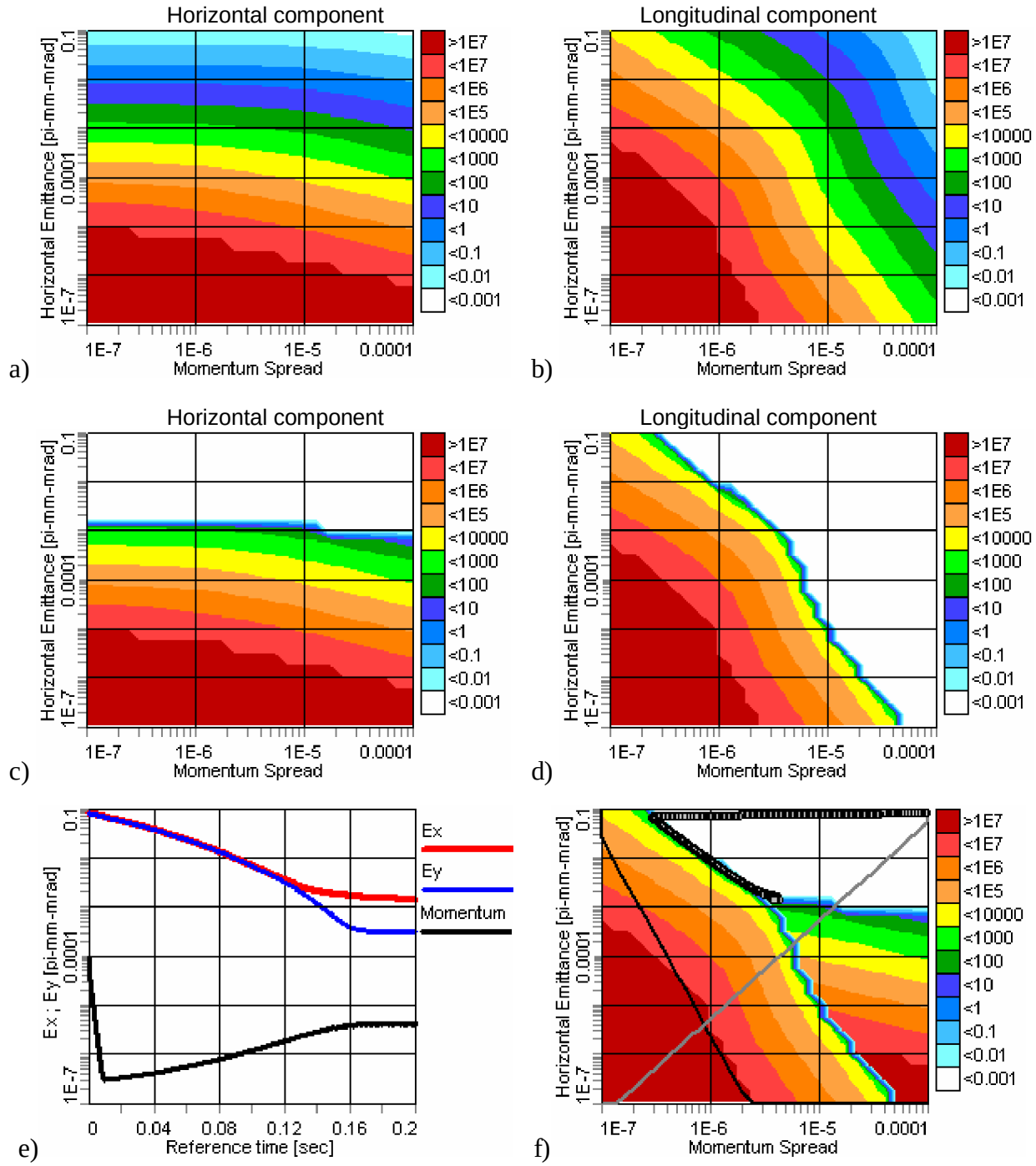

Fig.2.3. Growth rates for NAP-M (Martini model), $N_p = 10^6$, $I_e = 1$A.
a) horizontal component of IBS and **b)** longitudinal component of IBS (Martini model), **c)** horizontal component IBS+ECOOL, **d)** longitudinal component IBS+ECOOL, **e)** evolution of beam parameters (emittances and momentum spread) during cooling process, **f)** overlapping of **c** and **d** pictures and beam evolution from **e** and **f**. Gray straight line corresponds to equilibrium between transverse and longitudinal temperature, black straight line – ordering state criteria.

If the proton number is of 2×10^6 "the channel" between the IBS islands disappears on the summary picture (Fig.2.4,f) that means the ordered state can not be reached in this case. These results show that the ordered state of proton beam in NAP-M can be observed for particle number $\leq 10^6$. It means that experimental results with sudden reduction of momentum spread can not be explained by the ordering process.

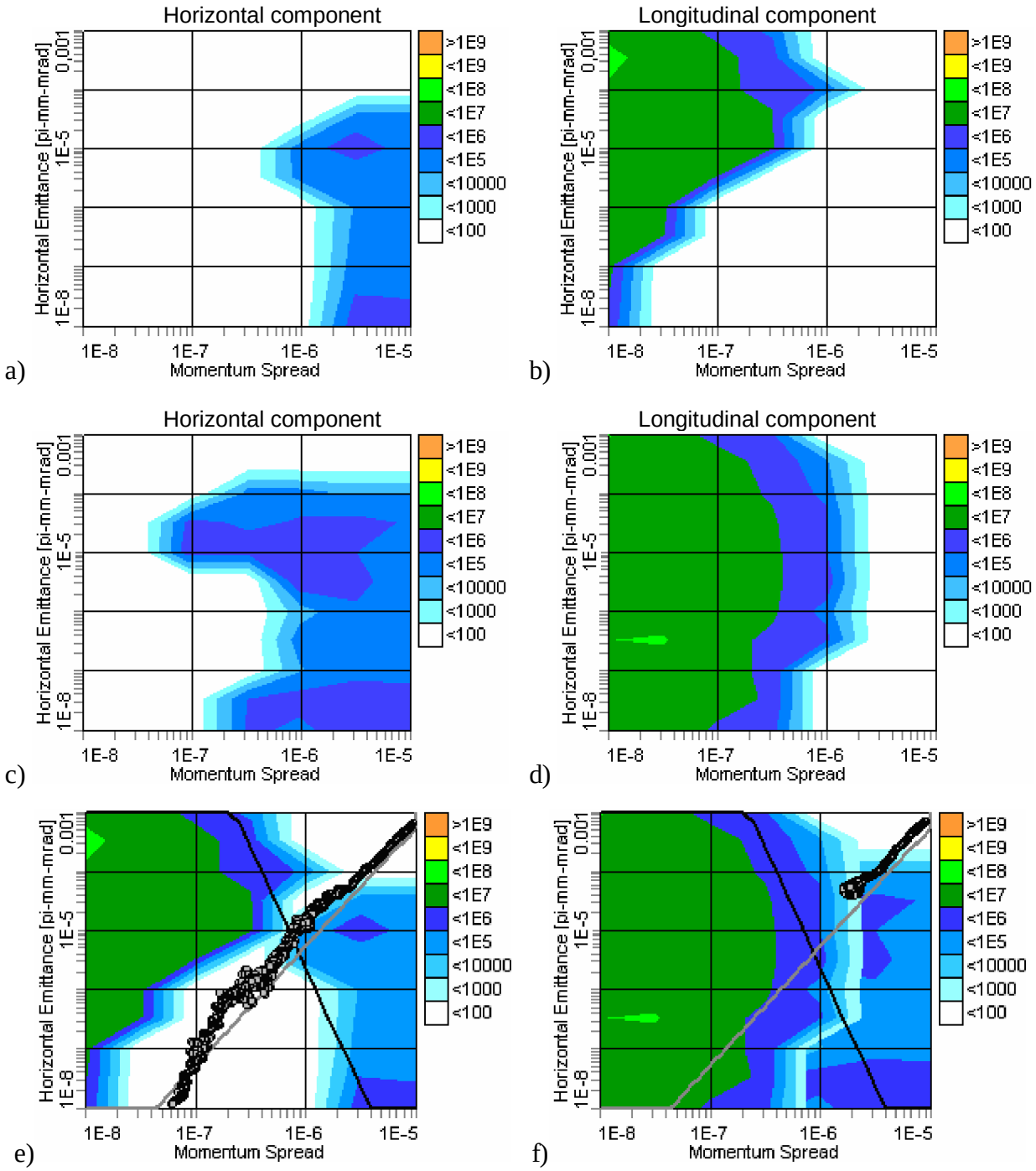

Fig.2.4. Growth rates for NAP-M (Molecular Dynamics).
a) horizontal component of IBS, $N_p = 10^6$, **b)** longitudinal component of IBS, $N_p = 10^6$,
c) horizontal component of IBS, $N_p = 2\times10^6$, **d)** longitudinal component of IBS, $N_p = 2\times10^6$,
e) evolution of beam parameters, $N_p = 10^6$, **f)** evolution of beam parameters, $N_p = 2\times10^6$.
Gray straight line corresponds to equilibrium between transverse and longitudinal temperature,
black straight line – ordering state criteria.

2.2. COSY simulation

COSY ring has the parameters similar to NAP-M at the injection energy (Table 2.2). This ring can be used for the study of the ordered proton beams. The main difference with NAP-M is the super periodicity of the lattice structure. NAP-M has the super periodicity equal to 4 (Fig.2.2), COSY lattice periodicity is equal to 1 (Fig.2.5).

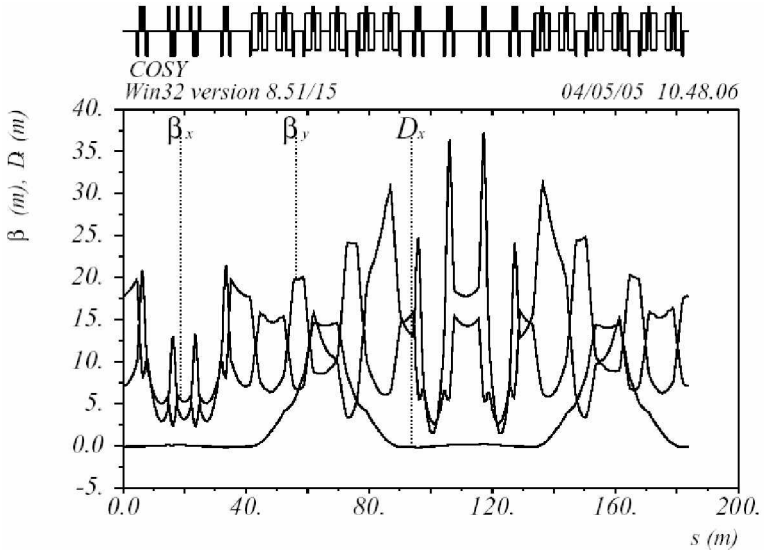

Fig.2.5. Lattice structure of COSY.

Table 2.2. Parameters of COSY.

Circumference, m	183,5
Proton energy, MeV	45,6
Transition energy, γ_{tr}	2,4
Betatron tunes, Q_x/Q_y	3,62 / 3,68
Dipole field stability	$\sim 2\times10^{-5}$
Electron cooler	
Cooling section length, m	1,4
Beam current, A	0 ÷ 1,0
Beam radius, cm	1,27
Magnetic field, kG	0,8
Electron energy stability	$\sim 2\times10^{-5}$

The theoretical and numerical (Fig.2.6,b) calculations of the longitudinal IBS growth rates have a large difference now from NAP-M lattice structure (Fig.2.6,d). The longitudinal component has a very specific IBS growth rate island in the region of transition point to ordered state. The same island was simulated for lattice structure of ESR and TARN2 also. The nature of this island is not explained yet. The experimental verification of this behavior of IBS growth rates at low temperature of ion beams is a very important task.

The numerical simulation techniques of the cooling process with Molecular Dynamics shows that the ordered state for COSY parameters can be reached if parameters of proton beam have special initial conditions: large transverse emittances and small momentum spread (Fig.2.6,e, the left “beam trajectory”).

If the proton beam trajectory starts at the equilibrium temperature (along gray straight line in Fig.2.6,e) then the proton beam reaches the equilibrium between cooling and heating and can not be cooled up to the ordered state.

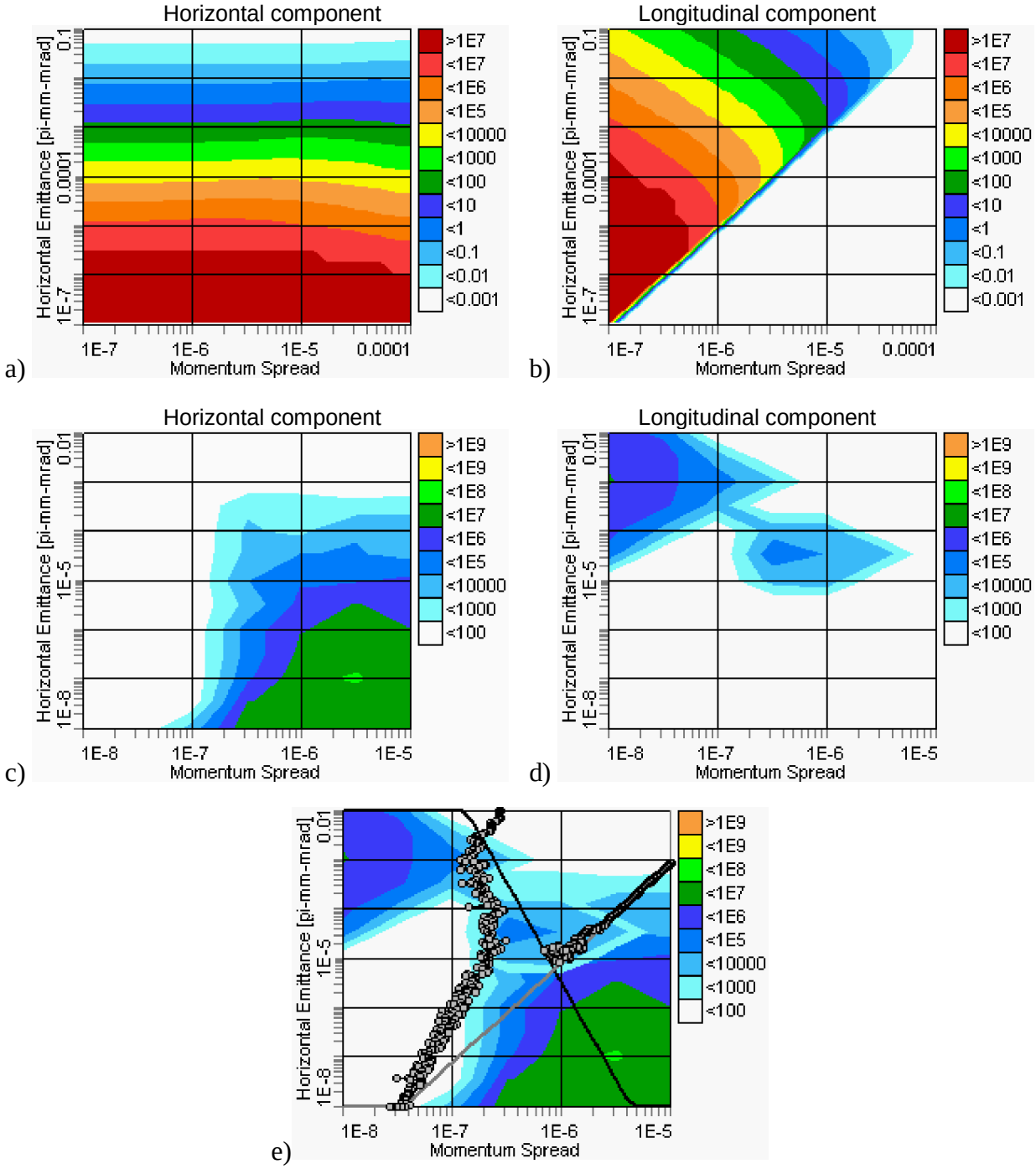

Fig.2.6. Growth rates of IBS and proton beam parameters evolution (gray squares) at electron cooling in COSY, $N_p = 10^6$.
a) horizontal component of IBS and **b)** longitudinal component of IBS (Martini model), **c)** horizontal component of IBS and **d)** longitudinal component of IBS (Molecular Dynamics), **e)** overlapping of **c** and **d** pictures and beam evolution during cooling process for different initial parameters. Gray straight line corresponds to equilibrium between transverse and longitudinal temperature, black straight line – ordering state criteria.

3. COSY experiments

3.1. Methods of the beam intensity and momentum spread measurement

The ordered proton beams were simulated at the injection energy (Table 2.2) and the lattice structure which corresponds to the experiments with the internal target (Fig.2.5). The experimental study of the cooling process of low intensity proton beam at COSY was done for the lattice structure presented in Fig.3.1. Simulation shows that the results of theoretical investigation do not depend significantly on the lattice structure.

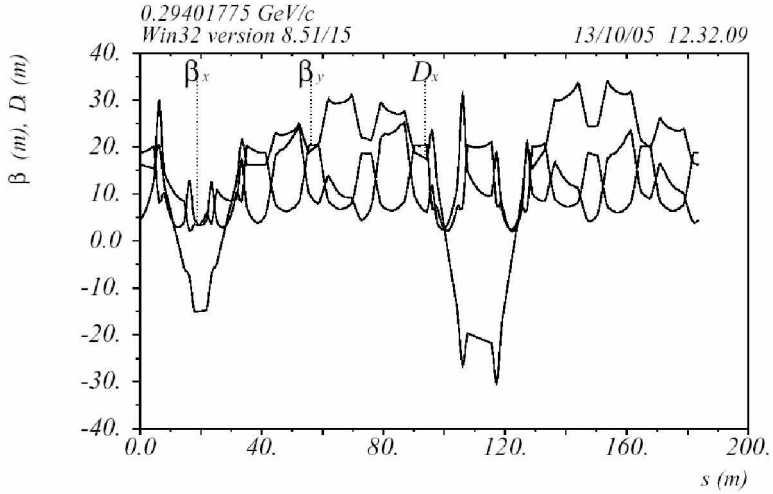

Fig.3.1. COSY Lattice structure at injection energy.

The proton beam momentum spread was measured after single injection as a function of time during decrease of the beam intensity at continuous electron cooling. The beam life-time at low intensity is determined mainly by proton single scattering on residual gas atoms on aperture. In the experiment the life-time was regulated by decrease of the ring aperture using horizontal or vertical scrapers.

The Schottky noise of the beam was detected using capacitive pickup electrodes. The amplifier was tuned for 18-th harmonics of revolution frequency (active filter). The shape of the Schottky noise spectrum is determined by collective phenomena and the beam momentum spread. The spectra amplitude $W(\omega)$ can be calculated in accordance with the formula [15]:

$$W(\omega) = G\frac{N_p(\Delta\omega n)^2}{2\pi\Omega_n^2}\frac{\mathrm{Im}\,\varepsilon}{\omega|\varepsilon|^2} \tag{3.1}$$

where G is a constant determined by the gain of the measurement system, N_p is the proton number, $\omega = 2\pi(f - nf_0)$ is the frequency shift at n-th harmonics of revolution frequency f_0, ε is a permittivity function, which can be written as the expansion:

$$\varepsilon = 1 + 2\frac{\Omega_n^2}{(\Delta\omega n)^2}\left[1 + \frac{i\omega}{\lambda q - i\omega}\left(1 + \sum_{m=1}^{\infty}\frac{q^m}{\prod_{i=1}^{m}(m + q - i\omega/\lambda)}\right)\right], \tag{3.2}$$

where $q = (n\Delta\omega/\lambda)^2$, λ - electron cooling decrement. $\Delta\omega$ - revolution frequency spread related to proton momentum spread as the following:

$$\Delta\omega = \omega_0 \eta \frac{\Delta p}{p}, \ \eta = \frac{p}{\omega}\frac{d\omega}{dp}, \tag{3.3}$$

Ω_n is a coherent frequency shift on *n*-th harmonics given by

$$\Omega_n^2 = (n\omega_0)^2 \frac{N_p r_p \eta \left(0.5 + \ln\frac{b}{a}\right)}{2C\gamma^3\beta^2}, \tag{3.4}$$

r_p is the proton classical radius, *b* and *a* are the vacuum chamber and beam radii correspondingly.

At a large proton number the shape of the spectrum has specific double peak structure. The measured shape can be fitted to theoretical dependence (3.1) by least-square method using cooling rate and momentum spread as fitting parameters. In the Fig.3.2 an example of the Schottky spectrum shape calculated in accordance with (3.1) at 10^8 protons, $2\cdot10^{-5}$ rms momentum spread and cooling increment of 80 s^{-1} is presented.

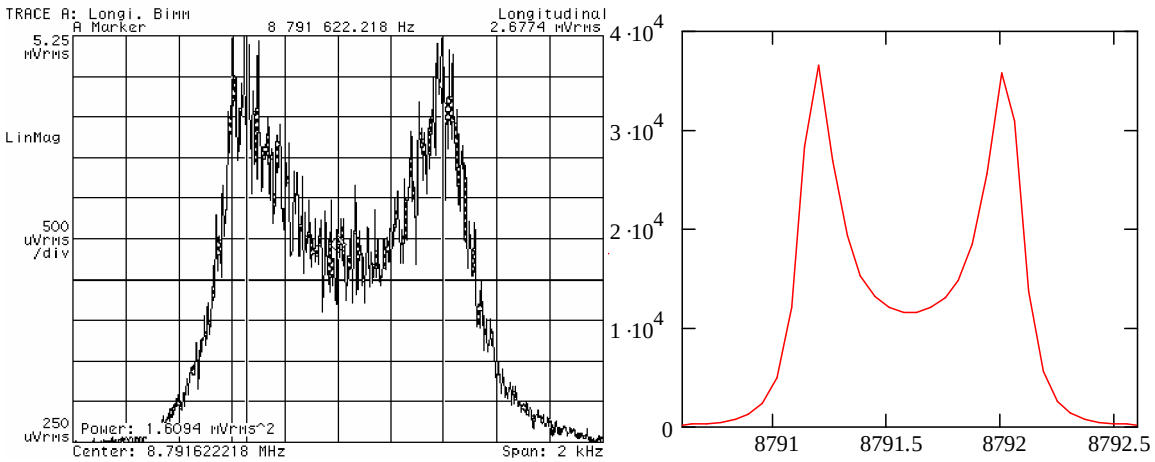

a) b)

Fig.3.2. Shape of the Schottky spectrum with two peaks. a) signal measured in the experiment, b) fitting curve in accordance with (3.1) - amplitude is in arbitrary units, frequency is in kHz, $N_p = 10^8$, $\Delta p/p = 2\cdot10^{-5}$, $\lambda = 80\ s^{-1}$.

At small proton beam intensity the Shottky spectrum becomes to be almost Gaussian, and the best fit is obtained by setting $\Omega_n = 0$ [10]. In this case the beam momentum spread can be calculated from measured frequency spread:

$$\frac{\Delta p}{p} = \frac{1}{\eta}\frac{\sigma_f}{n f_0} \tag{3.5}$$

Three methods for the measurement of proton number were used in the experiments:

1. Beam current transformer (BCT) monitor which measures the proton beam current,
2. H^0 monitor measuring the neutral atom flux from electron cooling section,
3. Schottky signal power.

Minimum sensitivity of BCT method is limited by the proton number of ~10^8. Amplitude of the signal from BCT monitor was measured with an oscilloscope. The proton number can be calculated with the following formula:

$$N_p = A_{BCT} \times 1.27 \cdot 10^8, \tag{3.6}$$

where A_{BCT} is BCT signal measured ib mV.

In the range of particle number $N_p = 10^8 \div 10^9$ this method and the second one (H^0 flux) are applicable and the signal from BCT monitor can be used for absolute calibration of H^0 monitor. The proton number can be found from H^0 count rate as the following (Fig.3.3):

$$N_p = 1.2 \cdot 10^6 * \hat{N}_{H0}[s^{-1}] \tag{3.7}$$

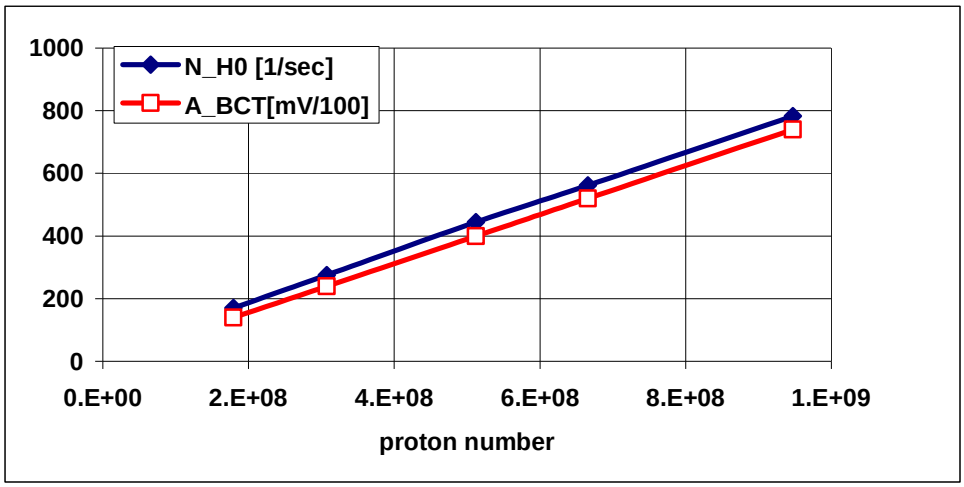

Fig.3.3. Calibration of H^0 monitor with BCT. I_e=250 mA.
N_H0 – number of H^0 particles per second, A_BCT – signal from beam current transformer.

Background noise for H^0 monitor is about 0.5 events per second. It limits the sensitivity of the monitor at the level of 5×10^5 protons. For smaller number of protons the Schottky signal power was used (Fig.3.4). In these experiments the Schottky signal was measured on 18-th harmonics of revolution frequency (f_{18}=8.7918 MHz). The value of Schottky signal power can be calculated with spectrum analyzer as one of its standard operations.

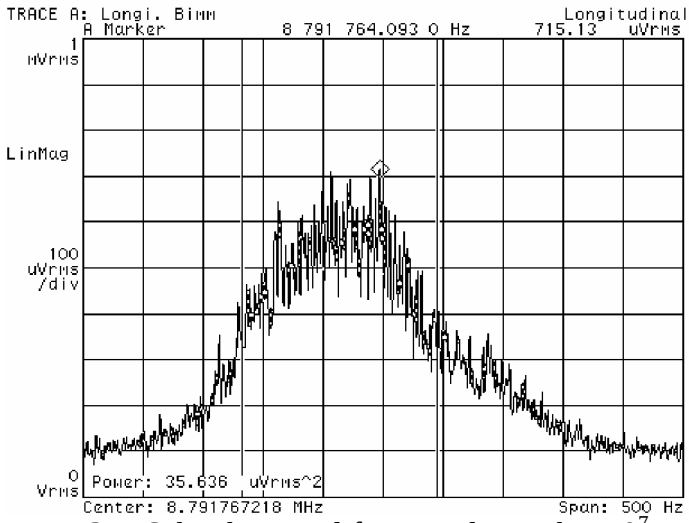

Fig.3.4. Schottky signal for particle number 10^7.

Calibration of the Schottky signal power $P_{Schottky}$ with H^0 monitor was done for the proton number in the range of $N_p = 10^6 \div 10^8$.(Fig.3.5). The calibration has given the relation between both parameters:

$$N_p = 4.5 \cdot 10^5 * P_{Schottky}[\mu V_{rms}^2] \tag{3.8}$$

The measurement of particle number with Schottky signal power could be used for proton number less than 10^6.

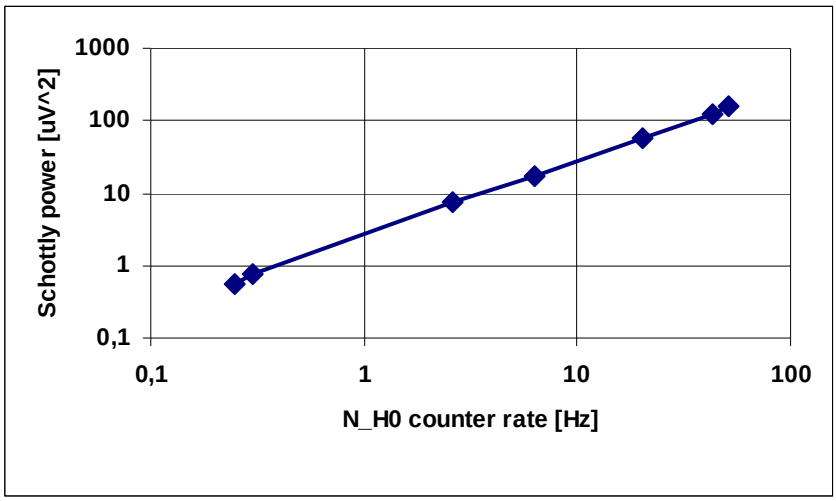

Fig.3.5. Calibration of Schottky signal power with H^0 monitor in COSY.

Proton number was measured in the wide range of N_p variation using of different methods. The dependence Full Width at Half Maximum (FWHM) of Schottky signal on particle number is presented in (Fig.3.6).

b)

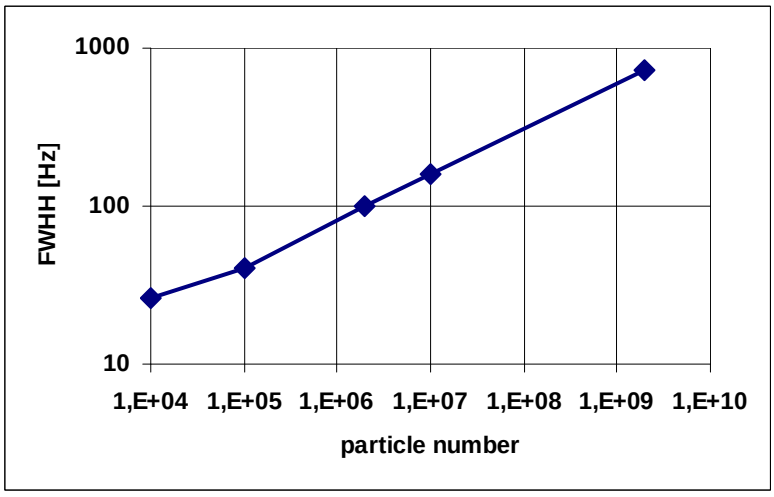

Fig.3.6. Dependence the width of the Schottky signal on particle number.

3.2. Equilibrium momentum spread of cooled proton beam

The aim of proposed experiments is achievement of ordered state for proton beam. The simulation has shown that the ordered state can be observed for proton number less than 10^6 and momentum spread less than 10^{-6} (Table 3.1). The stability of power supplies for dipole filed and

electron energy should be better than $1\div3\times10^{-6}$, the beam diagnostics has to measure the particle number below 10^5 and momentum spread down to value 10^{-6}.

Table 3.1. Required parameters for COSY experiment.

Storage ring particles	**NAP-M protons**	**ESR ions**	**COSY**	
			Before aug.05	**Required**
Circumference, m	47,25	108,36	183,5	
Proton/particle energy, MeV	65	270-400	45,6	
Transition energy, γ_{tr}	1,069	2,7824	2,4	
Betatron tunes, Q_x/Q_y	1,34 / 1,24	2,29 / 2,67	3,62 / 3,68	
Dipole field stability	$\sim10^{-5}$	2×10^{-6}	2×10^{-5}	$\mathbf{3\times10^{-6}}$
Electron cooler				
Cooling section length, m	1,0	1,8	1,4	
Beam current, A	0,300	0,25	0,3	**1,0**
Beam radius, cm	0,5	2,5	1,27	
Electron beam density, mA/cm^2	380	13	60	**200**
Magnetic field, kG	1,0	1	0,8	
Electron energy stability	$\sim10^{-5}$	1×10^{-6}	10^{-5}	$\mathbf{10^{-6}}$
Diagnostics / Sensitivity				
Beam current monitor, μA	1,0	~1,0	1,0	**1.0**
H^0 monitor, s^{-1}	10	---	1,0	**1.0**
Schottky noise detector, N_p	10^6	~10 (Z~50)	1×10^6	$\mathbf{3\times10^4}$

Electron cooling of the proton beam was done for the different values of electron beam current (Fig.3.7). Momentum spread was measured as FWHM (full width on half maximum) of the longitudinal Schottky signal when only one peak signal is observed. For larger number of protons after the cooling process the distribution of longitudinal Schottky signal has double peak structure and other method of momentum spread calculation is needed.

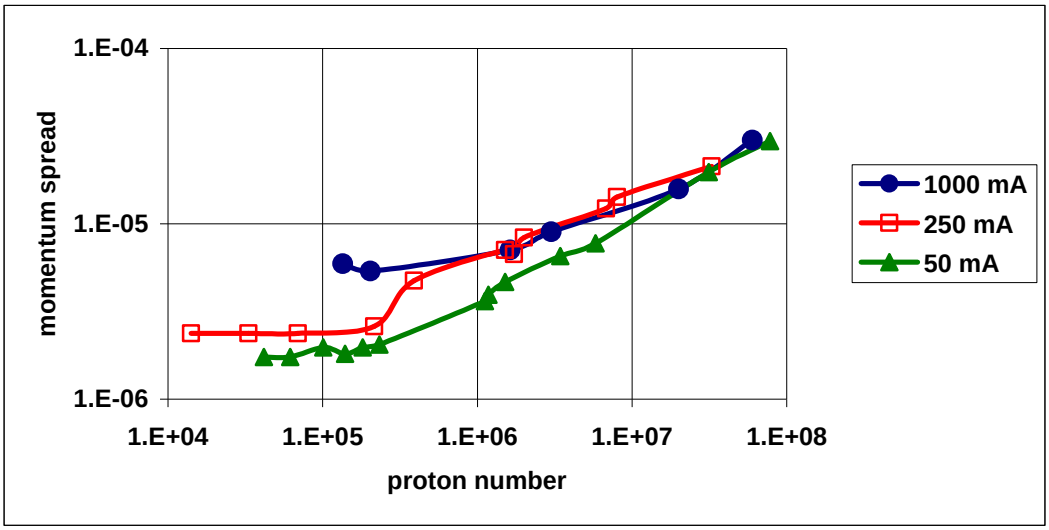

Fig.3.7. The dependence of momentum spread on the proton number for different values of electron beam current

In the experiments a measurement of dependence of $\Delta p/p$ on N_p was started with single injection of protons which filled the COSY ring with a new circulating beam of about $2 \div 5 \times 10^9$ protons. To speed up the process of proton loss the horizontal scraper was used. After a few minutes of the cooling process with inserted scraper the proton number decreases up to the value less than 10^8 and longitudinal Schottky signal transformed to a single peak. Then the scraper is returned to its initial position (full aperture) and the proton number continues to decrease with a constant lifetime.

When the proton number becomes less than 10^6 the momentum spread ends to decrease and has a constant value. No sudden reduction of momentum spread was observed in this experiment. It means that the proton beam does not achieve an ordered state at present parameters. Results of these experiments are very similar to those ones at NAP-M (Fig.2.1).

The COSY experiment results show that the minimum value of momentum spread depends on the electron beam current (Fig.3.8) and does not depend really on particle number in the range of $N_p \sim 10^5$. It means that the equilibrium state is defined by the parameters of the electron beam when intrabeam scattering is suppressed.

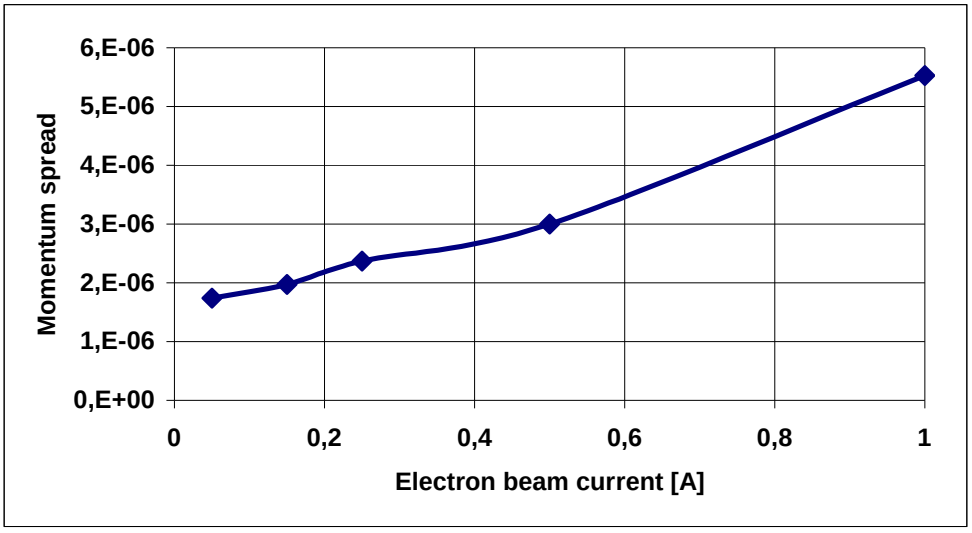

Fig.3.8. The dependence of minimum momentum spread on electron beam current.

To verify the simulation results which predict an existence of the island of the IBS longitudinal component (Fig.2.6,d) the additional transverse heating was applied to the proton beam. During the experiment the influence of two kind of heating was studied: the heating by “noisy” transverse electric field (signal of the spectrum close to white noise one (Fig.3.9) and heating via scattering on residual gas atoms.

The noise signal was applied to the electrodes of the beam position monitor. In the experiments this additional transverse heating resulted in increase of particle loss rate and at large proton number - to the excitation of beam resonances in the longitudinal direction (Fig.3.10). At a small proton beam intensity the heating did not lead to decrease of the equilibrium momentum spread.

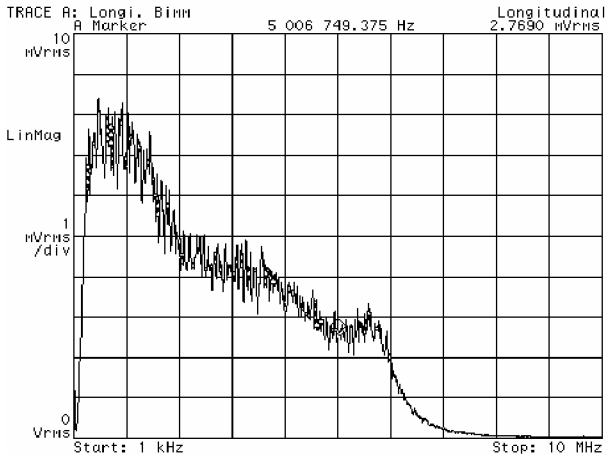

Fig.3.9. Spectrum of the noise signal used for the transverse heating of the proton beam.

Fig.3.10. Schottky noise spectrum at 10^7 proton number
(the same as in Fig.3.4) and transverse heating by white noise.

The proton beam heating with scattering on residual gas atoms was realized by increase of the nitrogen partial pressure in the vacuum chamber in the area of the ANKE target. The local pressure was increased more than by one order of magnitude; corresponding increase of the average pressure in the ring was about two times. Influence of the residual gas pressure and composition on the cooling process dynamics was not observed actually.

Conclusion

Simulations of the cooling process have shown that the proton beam parameters measured at NAP-M lies rather far from transition to an ordered state and the measured saturation of the beam momentum spread can not be explained with the beam ordering. At COSY one can expect the transition to the ordered state at rms momentum spread of about 10^{-6} and proton number below 10^6. The transition can be observed if the equilibrium momentum spread is determined by effective velocity spread of electrons and other heating processes leading to longitudinal heating are negligible. To perform the transition at maximum proton number one needs to provide large enough beam emittance using additional heating of the beam in transverse direction.

During preparation for experimental study of the cooling process at low intensity of the proton beam the stability of cathode high voltage power supply was sufficiently improved. Sensitivity of the Schottky noise measurements was improved by application of active filter at 18-th harmonics of revolution frequency. The spectrum was averaged during a few minutes of measurements.

During experiments the method of the proton number measurement was developed and tested. Depending on the beam intensity the particle number can be measured by BCT signal, H^0 flux intensity or Schottky noise power. All the signals are in the linear dependence one from other in wide range of the beam intensity and one can use BCT signal for calibration of other methods. At minimum beam intensity only Schottky noise power can be used for measurements and minimum detected proton number in the COSY was 10^4.

Minimum momentum spread value was achieved at electron current of 50 mA and it is equal to about $2 \cdot 10^{-6}$. This value corresponds to temperature of the proton beam longitudinal degree of freedom equal to about 1 – 2 meV. The beam momentum spread reaches the minimum value at intensity of $2 \div 3 \cdot 10^5$ protons and does not change at further decrease of the proton number. The dependence of the momentum spread on the particle number is in qualitative agreement with results of NAP-M experiment.

The achieved equilibrium beam parameters are closed to theory prediction for transition of the proton beam at COSY into ordered state. However, the sudden reduction of the momentum spread was not observed. More probably the minimum achievable momentum spread of the proton beam is determined by thermal equilibrium with cooling electrons. Friction force measurements performed at COSY earlier had indicated that the effective electron temperature lies in the range of a few meV.

Effective velocity spread of electrons is determined by stability of the cathode voltage power supply and accuracy of the longitudinal magnetic field in the cooling section. At low electron current the present stability of the cathode voltage corresponds to electron longitudinal temperature below 0.5 meV. More probably that the electron beam effective temperature is restricted by the magnetic field accuracy and can be improved in the future experiments using correction coils.

In theory the maximum proton number in the ordered state increases with increase of the electron beam current. The measurements were performed at electron beam current from 50 mA to 1 A. The minimum equilibrium momentum spread corresponds to minimum electron current. That can be explaining by decrease of the cathode voltage stability with increase the current. To prove this explanation one needs to provide direct measurements of the cathode voltage at different currents.

Two methods of the beam heating in the transverse direction were tested. Heating power due to scattering with residual gas atoms is limited by requirements for the vacuum conditions at the position of the electron gun cathode. Increase the pressure to maximum attainable value does not affect practically the cooling process.

The beam heating by transverse electric field with white noise spectrum leaded to longitudinal instability down to 10^6 protons. It can be explain by transverse displacement of the beam orbit in the position of the pickup electrodes. To improve efficiency of the transverse heating

one can increase of the noise bandwidth (for instance, to stabilize the beam emittance in Recycler ring at Fermilab the beam heating was provided by stochastic cooling system).

Acknowledgments

We are grateful to K.Henn, I.Mohos and D.Prasuhn for helping of experiments on COSY.

References

[1] R.Maier, “Cooler Synchrotron COSY – performance and perspectives”, NIM A 390 (1997) 1-8.
[2] http://lepta.jinr.ru/betacool.htm
[3] G.I.Budker, N.S.Dikansky, V.I.Kudelainen et al., Proc. 4th All-Union Conf. on Charged-Particle Accelerators [in Russian], Vol. 2 (Nauka, Moscow, 1975) 309; Part.Accel. 7 (1976) 197; At.Energ. 40 (1976) 49. E.Dementev, N.Dykansky, A Medvedko at al., Prep. CERN/PS/AA 79-41, Geneva (1979).
[4.] T. Katayama et al., MUSES Conceptual Design Report, RIKEN, November 2000
[5] R. Hasse, J. Schiffer. "The Structure of the Cylindrical Confined Coulomb Lattice". Annals of Physics **203** (1990) p.419.
[6] An International Accelerator Facility for Beams of Ions and Antiprotons, Conceptual Design Report, http://www.gsi.de/GSI-Future/cdr/PDF/S2_Kap1.pdf
[7] I. A. Koop, Conceptual Design for e-RI Collider Experiments at the NESR, Proceedings of the International workshop on Rare Isotope Physics at Storage Rings, Hirschegg, February 3-8, 2002
[8] M. Steck, K. Beckert, H. Eickhoff et al. Anomalous temperature reduction of electron-cooled heavy ion beams in the storage ring ESR. Phys.Rev.Lett., v.77 (1996) p.3803.
[9] R. W. Hasse, M. Steck. Ordered ion beams. Proceeding of EPAC'2000.
[10] H. Danared, A. Kallberg, K.G. Rensfelt, A. Simonsson. Observation of ordered ion beams in CRYRING. Proceeding of PAC'2001.
[11] U. Schramm, T. Schats, D. Habs. In Proc. Conf. on Appl. of Acc. in Research and Industry (eds J.L.Duggan) AIP Conf. Proc. p.576 (to be published).
[12] I.Meshkov, A.Sidorin, A.Smirnov, E.Syresin, T.Katayama, H.Tsutsui, D. Möhl. Simulation Study of Ordered Ion Beams. Preprint RIKEN-AF-AC-42, July 2003.
[13] I.Meshkov, A.Sidorin, A.Smirnov, E.Syresin, T.Katayama. Ordered State of Ion Beams. Preprint RIKEN-AF-AC-40, May 2002
[14] Parkhomchuk V.V. Proc. Of Workshop on Electron Cooling and Related Applications, Kernforschungszentrum Karlsruhe (1984) p. 71.
[15] Parkhomchuk V.V., Pestrikov D.V., Thermal noise of intensive beam in storage ring, Russian Journal of Technical Physics, Vol.50, N7, p.1411, 1980.